*Desalination and Water Treatment*
www.deswater.com
doi: 10.5004/dwt.2021.27536

233 (2021) 377–386
September

# Biosorption of Levafix brilliant blue dye using dried *Saccharomyces cerevisiae*: kinetics, equilibrium, and thermodynamic assessment

Hatice Ataçağ Erkurt, Joshua Tunde Olaifa*

*Faculty of Engineering, Cyprus International University, Haspolat, Nicosia via Mersin 10, Turkey, emails: joshuatunde17@gmail.com (J.T. Olaifa), herkurt@ciu.edu.tr (H.A. Erkurt)*

Received 1 February 2021; Accepted 23 June 2021

**ABSTRACT**

In the last decade, *Saccharomyces cerevisiae* has been considered for the biosorption of dye because of its availability, unique nature, and capacity for dye sorption. In this study, dried *S. cerevisiae* was studied for the biosorption of Levafix brilliant blue (LBB) dye. Influence of operational parameters such as solution pH, temperature, initial dyes concentration, adsorbent dose, and contact time was examined. Optimization of operational parameters shows that optimum concentrations for maximum LBB sorption by *S. cerevisiae* was 100 mg/L after 10–15 min at pH 3, and yeast biomass of 0.05 g at 30°C–45°C. Equilibrium, kinetics, and thermodynamics studies were conducted for the biosorption of the dye onto heat pretreated yeast biosorbent. The obtained data from the experiment were analyzed utilizing four isotherm models. The Langmuir isotherm presented the best performance with the calculated values of biosorption capacities of 83.33, 172, 99, and 66.70 mg $g^{-1}$ for the temperatures of 25°C, 30°C, 40°C, and 50°C respectively, demonstrating that too high temperature has a negative effect on the biosorption capacity of LBB. Biosorption kinetics were determined utilizing three kinetic models and it was revealed that the biosorption follows the pseudo-second-order model with a correlation coefficient as high as ($R^2$ = 1). The thermodynamic examination of the test demonstrated the procedure was feasible and unconstrained and the biosorption was controlled by the physisorption process as shown by the $\Delta G$ values in the range of 0 and 20 kJ/mol. The highest value of $E$ gotten from the D–R isotherm model was 0.4 kJ/mol which further confirm that the biosorption was control by physical process. Thus, the obtained results suggest that inactive *S. cerevisiae* can be an efficient and cheap option to expensive activated carbon for the treatment of dye wastewater.

*Keywords:* Biosorption; *Saccharomyces cerevisiae;* Levafix brilliant blue dye; Kinetics; Equilibrium; Thermodynamics

## 1. Introduction

In the textile industry, upto 2.8 billion liters is released as waste yearly in the process of dyeing and finishing. Babu et al. [1] documented that to color 1 kg of cotton with receptive dyes, 600–800 g sodium chloride, 0.3–0.6 kg dyestuff, and 70–150 L water are fundamental; the wastewater discharged has up to 20%–30% of the connected unfixed responsive dyes, high salt content, a normal grouping of 2,000 part per million (ppm), and coloring supplements. The discharge of these pollutants into the earth is repulsive as an outcome of genuine ecological issues connected with the dyestuffs and the result of their breakdown [2]. The textile industry expends a lot of water, fundamentally in the coloring and completing operations of the plants. In addition, the increased call for textile products and the relative increment in their production, couple with the use of engineered dyes have together added to dye wastewater getting to be noticeably one of the critical sources of serious contamination issues in momentum times [3,4]. Serious environmental

* Corresponding author.

pollution arise from the mixing of unused dyes in the run-off with water of pond, river or ground which may eventually lead to a severe health threat. Fishes in water bodies are given those textile dyes and we as humans take those fishes as one of the key elements of day-to-day foods. Numerous dyes are cancer-causing and influence the lifespan of aquatic organisms. Rahman et al. [5] reported that the level of aspartate aminotransferase (AST), serum creatinine (SCR), glutamate pyruvate transaminase (ALT), serum total bilirubin (STBI), serum urea (SBUN) were all found to be increased by both Levafix Blue CA and Levafix Amber CA.

Various method of textile wastewater treatment has been documented. These are broadly categorized to three: physical, chemical, and biological [6]. Physico-chemical strategies (such as electrokinetic coagulation, electrochemical treatment, membrane separation, electroflocculation solvent extraction, ion exchange, ozonation, irradiation, and katox treatment) are high-cost processes with low productivity, restricted flexibility, obstruction by other wastewater constituents and needs to treat the secondary waste generated. Adsorption with the use of activated carbon as an adsorbent for the removal of diverse types of contaminants is effective; however, it is costly. Therefore, adsorbent based on natural materials are more attractive and their efficacies have been broadly reported for the adsorption of different types of dyes. For instance [7], efficiently used a biocomposite comprising alginate, carboxymethyl cellulose, polyvinyl alcohol, and rice husk to remove various dyes from aqueous solutions [8]. In another study synthesized and characterized into two different composites, that is of sugarcane bagasse/zinc aluminum and apple peel/zinc aluminum biocomposites for the effective removal of reactive and acid dyes while the acid black dye was removed in a closely related investigation by Rahman et al. [9].

Biosorption is known as a metabolically latent process, which means it does not require energy, and the measure of contaminants a sorbent can effectively evacuate depends on motor balance and the piece of the sorbents cell surface [10]. The use of agro-industrial residue was as biosorbent for pollutant removal from aqueous solution has been further documented [11]. Atrazine was removed from an aqueous solution with the use of biosorbent made from seed husks of *Moringa oliefera*. The result of the suggest residues such as *M. oleifera* seed husk is a viable candidate for biosorbent preparation with the highest adsorption capacity 10.321 mg $g^{-1}$ at 318 K [11]. The huge favorable circumstance of this process is its low cost and reduced pollution [12]. Treatment of metals such as aluminum by *S. cerevisiae* was documented by various researchers. Using *S. cerevisiae* as a biosorbent has numerous advantages. Firstly, the biosorbent material is a by-product of various food and beverages industries, secondly, it is easy and cheap to grow using unsophisticated fermentation technique, thirdly, *S. cerevisiae* is a perfect model to distinguish the system of biosorption in color removal. Fourthly, *S. cerevisiae* is a eukaryotic microorganism with a high specific growth rate which is very important in preparing biosorbent in a short period time numerous studies on the use of *S. cerevisiae* has been presented in the literature, the use of *S. cerevisiae* to remove LBB dye from aqueous solution has not been studied. In this perspective, this study aimed not only to evaluate the potential use of *S. cerevisiae* for the elimination of LBB but also to proficiently adjust the physicochemical parameters as well as examining the mechanism of adsorption through kinetic, isotherm, and thermodynamic studies.

## 2. Materials and methods

### 2.1. Instruments

A bench-top centrifuge (ZENTRIFUGEN 2205 A, Germany) was used for phase separation. The samples were shaken in a water bath (SARTORIUS AG, GFL1083, Germany) at 150 rpm, dye concentrations during the course of sampling time were measured by a UV-visible spectrophotometer (Shimadzu). Microsoft excel 2010 was utilized for the graphical investigation of the acquired information. A Fourier transform infrared spectrometer (Shimadzu-IRPRESTIGE – 21) working in the range of 500–4,000 $cm^{-1}$, and with a universal ATR sampling accessory was used to determine functional groups of the *S. cerevisiae*.

### 2.2. Dyes and reagents

LBB which is a regularly utilized dye in the material industry was collected from the Environmental Engineering Laboratory of Cyprus International University, North Cyprus. 0.1 g powdered dyestuff was diluted in 100 mL of distilled water to prepare 1 g/L stock dye solution. In biosorption experiments, dilutions of the stock solution were used. All chemicals used in the experiments were analytical grade.

### 2.3. Biosorbent

*S. cerevisiae* or baker's yeast was purchased locally at Lemar market, CIU. It was incubated on a shaker (150 rpm, 30°C) in 20% glucose solution for 24 h. Cells were then harvested by centrifuging at 6,000 rpm for 10 min. The supernatant was discarded and the precipitate was further filtrated using a vacuum pump. The resulting biomass was rendered inactive by autoclaving for 12 h at 60°C. The heat pretreated biomass was collected and ground into fine particles. The obtained pretreated powdered yeast was stored in the refrigerator and used as biosorbent in the experiment.

### 2.4. Analytical methods

In order to know the maximum wavelength absorbance of LBB, 50 mg/L of the dye, the solution was taken and scanned by using a UV-Vis spectrophotometer and the maximum absorbance wavelength ($\lambda_{max}$) was observed to be 598 nm. A calibration curve was prepared by using the standard LBB dye solutions with known concentrations. Absorbance values were recorded at $\lambda_{max}$ of the dye and they were converted into concentration values by using the equation of the calibration curve.

### 2.5. Batch adsorption experiments

The batch adsorption trials were carried out in a progression of a conical flask of 250 mL capacity. In all the

experiments, the solution volume was 100 mL and the mixture of solution and the adsorbent was agitated by using a rotary incubator shaker at 150 rpm (GFL-1083 Model) for desired time. The initial pH of the solution was estimated using an electronic pH meter by dropwisely adding 0.1 M HCl or 0.1 M NaOH before adding the biosorbent. After each adsorption trial, samples were taken at different time intervals and were centrifuged. The concentration of the remaining dye was estimated utilizing a UV-VIS spectrophotometer at $\lambda_{max}$ = 598 nm. All experiments were performed and the data collected was used in the data analysis. Therefore, the influence of various experimental conditions on the biosorption efficiency of *S. cerevisiae* was studied as follows. The influence of pH on the adsorption capacity of LBB dye by the adsorbent was studied at an initial concentration of the dye 100 mg/L for pH values at 3, 4, 5, 6, 7, and 8 using 0.05 g of the biosorbent in 100 mL of the solution at 30°C. The test solutions were shaken at agitation speed 150 rpm for an hour in order to find out the effective pH for the dye sorption. The influence of adsorbent dose was investigated by adding different amounts (0.05, 0.1, 0.25, 0.5, and 1 g) of the biosorbent to determine the biosorbent dose for the highest dye removal. The influence of initial dye concentrations was examined by using different dye concentrations (25, 50, 75, 100, 150, and 250 mg/L) with the constant amount (0.1 g) of the pretreated yeast. The pH of samples was adjusted to pH 3.0 before adding the heat pretreated yeast cells. The test solutions were removed from the shaker at known time intervals. The adsorption capacity of the biosorbent was calculated by the Eqs. (1) and (2) and decolourization efficiency was calculated by Eq. (3).

$$Q_e = \frac{(C_0 - C_e)V}{m} \tag{1}$$

$$Q_t = \frac{(C_0 - C_t)V}{m} \tag{2}$$

$$\text{Decolourization efficiency}(\%) = \frac{C_0 - C_e}{C_0} \times 100 \tag{3}$$

where $Q_e$ and $Q_t$ is the adsorption capacity (mg/g) at the equilibrium and time $t$, respectively; $C_0$, $C_e$ and $C_t$ are the concentration of the dye in the solution (mg/L) at the initial, equilibrium and at time $t$, respectively; $V$ is the volume of the solution (L); and $m$ is the dry weight (g) of the biosorbent.

### 2.6. Adsorption isotherm, kinetic study, and thermodynamic study

The relationship between the amount of dye adsorbed and the residual dye concentration is well described by isotherm models [13]. Langmuir, Freundlich, Dubinin–Radushkevich (D–R), and Temkin models were tested for fitting the experimental data. For kinetic study, the pseudo-first, pseudo-second, and Weber Morris kinetic models were used to study the mechanism controlling the sorption process such as diffusion control, mass transfer, and chemical reaction. Adsorption thermodynamic studies were also done in order to deduce the biosorption mechanism of LBB on *S. cerevisiae* for varying temperatures (298–323 K).

### 2.7. Fourier-transform infrared spectrometry analysis

The functional groups of organic materials which allowed for the binding of the dye to the cell of the yeast cell were studied with a Fourier-transform infrared spectrometer (Shimadzu-IRPRESTIGE – 21) in the frequency range of 500–4,000 $cm^{-1}$ and with a universal ATR sampling accessory to determine functional groups of the *S. cerevisiae*.

## 3. Result and discussion

### 3.1. Effect of pH

The solution pH influences the solubility of the adsorbate, that is dye, the functional groups of the biosorbent (yeast) cell wall. The effect of pH on LBB biosorption using *S. cerevisiae* was investigated by adjusting the pH between pH 3 and 7. Fig. 1 reveals the variation in the concentration of adsorbed dye at varying initial pH values. From Fig. 1, it is obvious that % removal and amount adsorbed ($q$) significantly reduced with increasing pH from 3 to 7. At pH 3, the dye adsorption capacity was 109 mg/g, with 94% decolorization efficiency. These values decreased considerably to 65 mg/g and 54%, respectively at pH 4. This reduction continued gradually as the pH value increased up to 7.

The results showed that pH can be said to be a vital factor affecting the biosorption process. It can be attributed to the segregation of functional groups on the functioning sites of the biosorbent as well as the chemical conformation of the dye molecules in water and the changes of surface charge of the biosorbent [14]. It was found that adsorbed amount of dye goes down invariably with the increasing pH of the solution but increases with time. The cell wall of *S. cerevisiae* contains various functional groups such as amine, carboxyl, acidic polysaccharides, amino acids, and

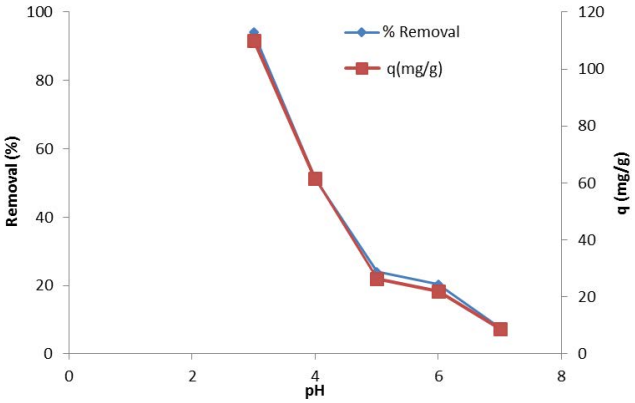


Fig. 1. Effect of pH on biosorption capacity and removal efficiency of LBB on *Saccharomyces cerevisiae* at equilibrium (100 ± 20 mg/L initial dye concentration, 30°C, 0.05 g biosorbent dose).

lipid groups. Hence, the predominant charges on the cell wall of *S. cerevisiae* are positive and due to anionic dye species, the superior mechanism of biosorption seems to be electrostatic attraction [15]. At pH 3, high extensive fascination occurs between the negatively charged anionic dyes molecules and positively charged cell surface. An increase in negative charge of *S. cerevisae* biomass with an increasing pH values was reported as well [16]. As the pH value increases, the biosorption of LBB on *S. cerevisiae* biomass tends to decrease, this can be ascribed to the increase in electrostatic repulsion between the negatively charged sides of the biomass and the anionic dye solution [17]. A comparable perception was made for LBB biosorption on inactive *Aspergillus oryzae* [18] and also for Remazole Blue dye biosorption on *S. cerevisie* [19].

Acidic reactive dyes are generally decolorized at lower pH values whereas basic reactive dyes are removed at higher pH values [20]. It can also be explained that lower pH values results in an increase in hydrogen ion concentration which also functions as bridging ligand between yeast cell wall and dye molecule, hence making more amount of anionic dye sorption occur [21,22].

### 3.2. Effect of temperature

The influence of temperature on biosorption by *S. cerevisiae* is shown in Figs. 2 and 3. The results showed that change in temperature does not affect the biosorption of LBB by *S. cerevisiae* as no significant increase or decrease in the biosorption capacity of *S. cerevisae* was observed with change in temperature. However, it can be clearly seen in Fig. 2 that the optimum temperature for this process is 30°C–40°C. This condition (30°C–40°C) is where the maximum dye removal (92%) was observed. As the temperature was additionally expanded to 50°C, a slight diminishing in adsorption was noticed, similar results were also reported for Ramazole Blue dye on eucalyptus barks where adsorption decreased at higher temperatures [23]. The slight reduction in biosorption as a result of increasing temperature may be ascribed to stronger bonds being formed at lower temperature supporting the fact that the adsorption is exothermic [24].

Generally, decolorization of LBB was efficient at a wide range of temperatures (25°C–50°C). This result indicates that higher temperature does not alter the structure of biosorbent [18]. A similar result was observed when inactive *A. niger* was used to decolorize LBB [18]. According to Benguella and Benaisa [25], the sorption rate goes up via ion or particle diffusion with an increase in temperature. However, the data gotten from this investigation show that dye ion diffusion is not the rate-restricting step of biosorption, therefore an increase in temperature did not significantly affect the diffusion processes. The results of this study further confirm that adjustment in temperature does not influence biosorption ability [26].

### 3.3. Effect of dose of biosorbent

The influence of biosorbent dose was also investigated on the biosorption of LBB. It can be seen from the graph that as the biosorbent dosage increases, decreases in dye uptake was observed. In other words, the lower the dosage of the biosorbent used, the higher the biosorption capacity (mg/g). The biosorbent dosage with the highest biosorption capacity was found to be 0.05 g (97 mg/g), followed by 0.1 g (80 mg/g) while the least biosorption capacity was recorded using 1 g (9 mg/g) which is the highest biosorbent dose used in this experiment (Fig. 4). On the other hand, an increase in biosorbent dosage brought about an increase in percentage of dye removal (Fig. 4). The maximum percentage of dye removal was observed with 1 g biosorbent dosage (92%), followed by 0.5 g (85%) while the least percentage dye removal was observed with 0.05 g biosorbent dosage (45%). The result of this investigation could be attributed to the relationship between the color ion and the coupling locales of the biosorbent. An increment of electrostatic interaction at high biomass fixation could inhibit dye molecule absorption. At low biomass dosage, dye molecules in the solution will enter into the intracellular part, thereby enhancing the concentration gradient of the dye molecule. It can be said that biosorption capacity is enhanced with an increase in inter-cellular distance (low biosorbent dosage). Mahmoud [16] observed an increase in biosorption

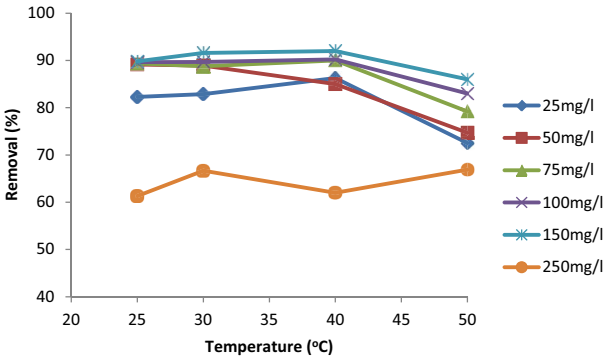


Fig. 2. Effect of temperature on LBB removal efficiency for different initial dye concentrations at equilibrium time and pH 3, 100 mg/L ± 20 initial dye concentration, 30°C temperature, 0.05 g biosorbent dose.

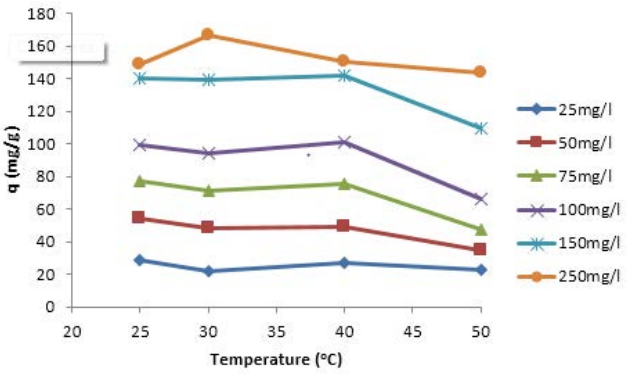


Fig. 3. Effect of temperature on LBB biosorption on *S. cerevisiae* at different initial dye concentrations at equilibrium time and pH 3, 100 mg/L ± 20 initial dye concentration, 30°C temperature, 0.05 g biosorbent dose.

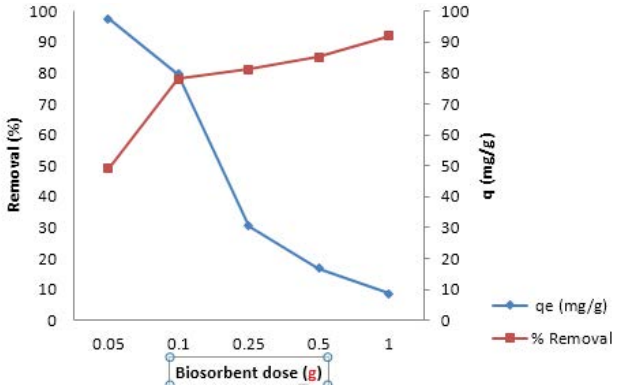


Fig. 4. Influence of biosorbent dosage on biosorption capacity and percentage dye removal (100 mg/L initial dye concentration, 30°C, pH 3).

capacity with decreasing biosorbent dose and increase in percentage dye removal with increasing biosorbent dosage when pine cone was used to decolorize certain reactive dye from aqueous solution. Similar results were also reported when *S. cerevisiae* and *R. nigricans* were used to adsorb reactive green dye in another investigation [27].

### 3.4. Effect of initial dye concentration

The dye initial concentration has a significant influence on the process of biosorption. The influence of different initial dye concentrations (25–250 mg/L) of LBB on biosorption was investigated for 60 min. Biosorption capacity was increased as the initial dye concentration was increased from 25 to 250 mg/L (Fig. 5).

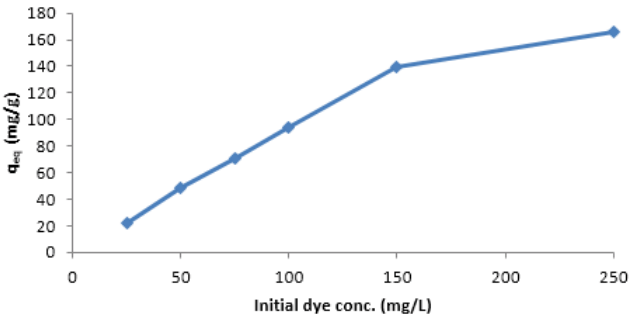


Fig. 5. Influence of initial dye concentration on equilibrium biosorption capacity (pH 3, 30°C, 0.05 g biosorbent dose).

The time required to reach equilibrium adsorption capacity was also noticed to expand with increasing dye concentration. Lower initial dye concentrations seem to reach equilibrium faster when compared to higher dye concentrations. A similar result was obtained when inactive biomass of *A. niger* was used to decolorize LBB [18].

### 3.5. Adsorption isotherm studies

Different isotherm models were studied for the biosorption of LBB onto pretreated *S. cerevisiae* (Table 1). Langmuir, Freundlich, Dubinin–Radushkevich (D–R), and Temkin models were used to characterize the adsorption equilibrium in this study.

#### 3.5.1. Langmuir model

The model depends on the presumption that adsorption occurs on a single layer of the uniform surface

Table 1
Langmuir, Freundlich, Dubinin–Radushkevich, and Temkin isotherm constants for the adsorption of LBB on *Saccharomyces cerevisiae*

| Isotherm model | Parameters | Temperature (°C) | | | |
|---|---|---|---|---|---|
| | | 25 | 30 | 40 | 50 |
| Langmuir | $Q^0$ (mg/g) | 83.33 | 172 | 99.00 | 66.70 |
| | $B$ (L/mg) | 0.05 | 0.047 | 0.050 | 0.060 |
| | $R_L^*$ | 0.4 | 0.3 | 0.17 | 0.14 |
| | $R^2$ | 0.9250 | 0.9906 | 0.9938 | 0.9119 |
| Freundlich | $K_F$ (mg/g) | 12 | 9.8 | 2.5 | 7.5 |
| | $1/n$ | 0.65 | 0.70 | 1.60 | 0.75 |
| | $N$ | 1.5 | 1.43 | 0.63 | 1.3 |
| | $R^2$ | 0.8750 | 0.9110 | 0.9901 | 0.8059 |
| Dubinin-Radushkevich (D–R) | $q_m$ | 241.10 | 246.20 | 3962.2 | 23.70 |
| | $Q_{D-R}$ (mg/g) | 114.6 | 100.4 | 152.3 | 131.7 |
| | β (mol²/kJ²) | 0.0011 | 0.0008 | 0.0004 | 0.0005 |
| | $E$ (kJ/mol) | 0.02 | 0.03 | 0.04 | 0.03 |
| | $R^2$ | 0.8009 | 0.9261 | 0.9681 | 0.9633 |
| Temkin | $A_T$ (L/mg) | 0.3 | 0.3 | 0.26 | 0.23 |
| | $b_T$ | 47.40 | 47.73 | 24.32 | 52.10 |
| | $B$ (J/mol) | 52.30 | 52.80 | 107.00 | 52.10 |
| | $R^2$ | 0.9305 | 0.9932 | 0.9107 | 0.9871 |

meaning that there is no cross interface between adjacent adsorbed molecules when alone molecule occupies a single surface site. This implies that all the active sites are energetically the same. The model is given as:

$$q_e = \frac{q_m b C_e}{1 + bC_e} \tag{4}$$

Changing Eq. (4) into Eq. (5) for linearization,

$$\frac{1}{q_e} = \frac{1}{bq_m}\frac{1}{C_e} + \frac{1}{q_m} \tag{5}$$

where $C_e$ is the equilibrium concentration of adsorbate (mg/L), $q_e$ is the measure of sorbate adsorbed per gram of the adsorbent at equilibrium (mg/g), $q_m$ is the maximum monolayer sorption capacity (mg/g), $b$ is the Langmuir isotherm constant (L/mg). The values of $q_m$ or $Q^0$ maximum adsorption capacity of biosorbent are obtained from the $1/q_e$ vs. $1/C_e$ graph. The important attribute of Langmuir isotherm is revealed as $R_L$ (a constant with no dimension) which is known as the separation factor. $R_L$ can be estimated by using Eq. (6).

$$R_L = \frac{1}{1 + bC_0} \tag{6}$$

The value of $R_L$ shows the type of the isotherm to be irreversible ($R_L$ = 0), favorable (0 < $R_L$ > 1), linear ($R_L$ = 1), or unfavorable ($R_L$ > 1). The regression coefficient ($R^2$) of Langmuir model for all the temperatures are closer to 1 and higher than Freundlich model. The monolayer maximum adsorption capacity estimated from Langmuir for 40°C and 50°C are 99 and 66.7 mg/g, respectively. The closeness of these values to experimental data (101.3 and 66.3 mg/g) for both 40°C and 50°C suggest good application of Langmuir model for his experiment. Likewise, the $R_L$ of LBB adsorption which ranges from 0.14 and 0.4 is a good indication that the biosorption of LBB onto *S. cerevisiae* is favorable.

### 3.5.2. Freundlich isotherm

Freundlich isotherm model is mostly used to show the adsorption characteristic of a heterogeneous surface; the isotherm is thereby derived to model multi-layer adsorption. The Freundlich isotherm model is expressed by Eq. (7).

$$q_e = K_F C_e^{1/n} \tag{7}$$

Eq. (8) is obtained by linearizing Eq. (7).

$$\ln q_e = \ln K_F + \frac{1}{n}\ln C_e \tag{8}$$

where $K_F$ is the Freundlich isotherm adsorption capacity constant (mg/g); $n$ is the adsorption force; $C_e$ is the equilibrium concentration of adsorbate (mg/L). $q_e$ is the measure of metal sorbate adsorbed per gram of the adsorbent at equilibrium (mg/g). $K_F$ and $1/n$ can be computed from the plot of $\ln q_{eq}$ against $\ln C_{eq}$. According to the isotherm, the value of $1/n$ between 0 and 1 for the biosorption process is considered good. From the data in Table 1, the adsorption process does not fit well to the Freundlich model as $R^2$ values are lower than the $R^2$ values obtained with the Langmuir isotherm model. Also, $n$ values exceed 1 except for 40°C.

The nature of adsorption result can be considered monolayer because $Q^0 > K_F$ for the four temperatures studied (Table 1).

### 3.5.3. Dubinin–Radushkevich (D–R) model

D–R isotherm model is used to indicate the mechanism of adsorption with a Gaussian energy distribution onto a heterogeneous surface, that is, D–R shows for the most part connected to decide the idea of adsorption process as physical or substance. The D–R condition is communicated as:

$$q_e = q_{\text{D–R}} e^{\beta\varepsilon^2} \tag{9}$$

Eq. (9) is linearized in Eq. (10).

$$\ln q_e = \ln q_{\text{D–R}} - \beta\varepsilon^2 \tag{10}$$

where $q_e$ (mol/g) is the amount of dye adsorbed on the adsorbent at equilibrium, $q_{\text{D–R}}$ (mol/g) is the maximum adsorption capacity; β (mol²/kJ²) is a coefficient related to the mean free energy of adsorption, and ε (J/mol) is the Polanyi potential which can be estimated as:

$$\varepsilon = RT\ln\left(1 + \frac{1}{C_e}\right) \tag{11}$$

The constant β gives an idea about the mean free energy $E$ (kJ/mol) of adsorption and it can be calculated by using Eq. (12).

$$E = \frac{1}{\sqrt{-2\beta}} \tag{12}$$

where $R$ is the gas constant (8.314 J/mol K), $T$ is the absolute temperature (°K) and $C_e$ is the adsorbate equilibrium concentration (mg/L). One of the particular attributes of D–R isotherm demonstrates and depends on the assurance that it is temperature-subordinate, which when adsorption information at various temperatures are plotted as a component of the logarithm of adsorption capacity at equilibrium ($\ln q_e$) vs. $\varepsilon^2$ (square of potential energy, if $E$-value is in the range of 8 and 16 kJ/mol then the adsorption procedure is considered to be chemical ion exchange and if $E$ < 8 kJ/mol, the adsorption is considered to be physical. The $E$-value for all the temperatures studied was found to be less than 8 kJ/mol showed that the adsorption procedure is physical adsorption.

*3.5.4. Temkin isotherm*

This isotherm model shows the relationship between the adsorbate and the adsorbent. By neglecting very low and high concentration values, the model accept that adsorption heat of all molecules in the layer would diminish linearly as opposed to logarithmic scope [28]. As suggested in the condition, its deduction is portrayed by a uniform conveyance of restricting energies (up to some most extreme restricting energy) was done by plotting the amount sorbed $q_e$ against $\ln C_e$ and the constants were computed from the slope and intercept. The model is expressed by Eq. (13) and it is lineralized in Eq. (14).

$$q_e = \frac{RT}{b}\ln\left(A_T C_e\right) \tag{13}$$

$$q_e = \frac{RT}{b}\ln A_T + \left(\frac{RT}{b}\right)\ln C_e \tag{14}$$

$$B = \frac{RT}{b_T} \tag{15}$$

$$q_e = B\ln A_T + B\ln C_e$$

where $A_T$ is the Temkin isotherm harmony restricting consistent (L/g), $b_T$ is the Temkin isotherm constant, $R$ is the gas constant (8.314 J/mol/K), $T$ is the temperature at 298°K. $B$ is the constant identified with the temperature of sorption (J/mol), the results from the table ($A_T$ = 0.23–0.3 L/g, $B$ = 52–107 J/mol and $R^2$ = 0.9107–0.9932) is a sign that the adsorption procedure was great for all the temperature.

*3.6. Kinetic studies*

What controls the adsorption kinetic is the rate with which molecules of dye are exchanged from the mass solution for the adsorbent surface. It provides an understanding the conceivable system of sorption, and the time taken for the sorbate particles to be adsorbed on the surface of the sorbent. As the adsorption procedure occurs in a stepwise progression mass movement is followed by boundary layer diffusion which is followed by the movement of sorbate within the pores of the biosorbent and lastly the sorption of the dye on the sorbent occurs. The first step is very quick under shaking conditions and the last step occurs very quickly as well. Second or the third step would be the rate-limiting step. With a specific end goal to recognize that and clarify the system of adsorption of LBB particles on *S. cerevisiae*, the kinetic studies were carried out by using kinetic models.

*3.6.1. Pseudo-first-order kinetic model*

This model is one of the first known to depict the rate of adsorption as regard adsorption capacity. It relies upon the presumption that the rate of adsorption is with respect to the amount of free restricting locales. Its linearized form is given by the formula:

$$\ln\left(q_e - q_t\right) = \ln q_e - k_1 t \tag{16}$$

where $q_e$ and $q_t$ are the adsorption capacity of adsorbent at equilibrium and at the time $t$, respectively (mg/g), $k_1$ is the pseudo-first-order rate constant ($min^{-1}$). The kinetic constants are computed from the slope and intercept of plot $-\ln(q_e - q_t)$ vs. $t$. The regression coefficient values ($R^2$) are viewed as a measure of the integrity of fit for the trial. $q_e$, $k_1$, and the regression coefficient values ($R^2$) are presented in Table 2. Low $R^2$ values indicate the inapplicability of the model to this framework.

*3.6.2. Pseudo-second-order kinetic model*

Pseudo-second-order model depends on the presumption that the degree of adsorption is corresponding to the square of the quantity of vacant binding sites [29]. Linearly, the model is represented as:

$$\frac{t}{q_t} = \frac{1}{kq_e^2} + \frac{1}{q_e t} \tag{17}$$

where $k_2$ is the pseudo-second-order rate constant ($min^{-1}$). The slope and intercept of the plot $t/q_t$ vs. $t$ give the estimation of $q_e$ and $k_2$ (Table 2), individually. $h$ (mg/g min) which describes the initial sorption rate can be calculated by the expression:

$$h = kq_e^2 \tag{18}$$

From Table 2, the $q_e$(calc) values are as close to $q_e$(exp) values for the adsorbent. Additionally, the coefficients got in this study for this model are higher (>0.99) for the temperatures than all other examined models proposing that the procedure can positively be portrayed by the second-order kinetic.

*3.6.3. Weber Morris kinetic model*

As indicated by this model, the plot of $q_t$ vs. $t^{1/2}$ ought to be linear ($C$ = 0) if intraparticle dispersion happens in the entire adsorption system and the intraparticle dissemination is the main rate constraining step of the procedure, in any case, if the line did not cross the root ($C \neq 0$) both intraparticle dispersion and limit layer impact both happens in the adsorption procedure. The model is shown in Eq. (19).

$$q_t = k_d t^{1/2} + C \tag{19}$$

where $k_d$ (mg/g $min^{1/2}$) is the rate constant of the Weber Morris model and $C$ is the intercept.

It can be seen from the table that $C \neq 0$ indicate that both intraparticle diffusion and boundary layer both influenced the biosorption of LBB on *S. cerevisia* and it also

Table 2
Kinetic parameters for LBB biosorption onto *S. cerevisiae* at different temperatures and pH

| Model and parameters | Temperature (°C) | | | | pH | | | | |
|---|---|---|---|---|---|---|---|---|---|
| | 25 | 30 | 40 | 50 | 3 | 4 | 5 | 6 | 7 |
| Pseudo-first-order | | | | | | | | | |
| $q_e$ (mg/g) | 2.41 | 1.20 | 1.61 | 2.50 | 1.20 | 15.8 | 6.6 | 5.7 | 5.5 |
| $k_1$ (min$^{-1}$) | 0.125 | 0.043 | 0.023 | 0.06 | 0.043 | 0.025 | 0.0045 | 0.0281 | 0.0055 |
| $R^2$ | 0.8275 | 0.5129 | 0.6668 | 0.6463 | 0.5129 | 0.8646 | 0.7562 | 0.7572 | 0.8485 |
| Pseudo-second-order | | | | | | | | | |
| $q_e$ (mg/g) | 94.34 | 110 | 102 | 66.67 | 110 | 64.1 | 27.1 | 22.9 | 8.7 |
| $k_2$ (min$^{-1}$) | 0.01 | 0.03 | 0.05 | 0.07 | 0.03 | $8.2 \times 10^{-3}$ | $7.5 \times 10^{-3}$ | 0.022 | 0.13 |
| $h$ (mg/g min) | 125 | 322.6 | 499.6 | 322.6 | 322.6 | 33.56 | 5.5 | 11.37 | 9.67 |
| $R^2$ | 1 | 0.9999 | 1 | 1 | 0.9999 | 0.9948 | 0.9583 | 0.9957 | 0.9867 |
| Weber–Morris | | | | | | | | | |
| $K_{id}$ (mg min$^{0.5}$/g) | 0.2 | 0.5 | 0.4 | 0.35 | 0.5 | 2.34 | 1.3 | 1.1 | 0.3 |
| $C$ | 92.8 | 106.07 | 98.8 | 64.24 | 106.07 | 46.13 | 15.3 | 15.00 | 6.80 |
| $R^2$ | 0.7677 | 0.5182 | 0.7875 | 0.7693 | 0.5182 | 0.5924 | 0.6044 | 0.5719 | 0.9332 |

reveals that intraparticle diffusion model was not only the rate-controlling step.

### 3.7. Adsorption thermodynamic

Thermodynamics studies were done to determine the mechanism of adsorption of LBB on *S. cerevisiae* for different temperatures (298–323 K). The thermodynamic parameters were computed using free energy change ($\Delta G$), enthalpy change ($\Delta H$), and entropy change ($\Delta S$) given by the following equations:

$$\Delta G = -RT \ln K_C \tag{20}$$

The enthalpy change ($\Delta H$) and entropy change ($\Delta S$) parameters were estimated from the equation below:

$$\ln K_C = \frac{\Delta G}{R} - \frac{\Delta H}{RT} \tag{21}$$

where $\Delta G$ is the Gibbs free energy change, $R$ is the universal gas constant (8.314 J/mol K), $T$ is the temperature (K) and $K_C$ ($q_e/C_e$) is the equilibrium constant. $\Delta H$ and $\Delta S$ in the biosorption process was gotten from a slope and intercept of the plot of $\ln K_C$ vs. $1/T$, respectively. The values of $\Delta H$, $\Delta S$, and $\Delta G$ were calculated using the equations above.

According to Table 3, the values of $\Delta H$ and $\Delta G$ were negative which shows that LBB biosorption is feasible and spontaneous. The positive values of $\Delta S$ also indicate enhanced randomness at the solid/liquid interface amid the adsorption procedure. According to the literature, $\Delta G$ values between the 0 and 20 kJ/mol are considered physisorption while the values between 80 and 400 kJ/mol are considered to be chemisorption [30]. $\Delta G$ calculated for *S. cerevisiae* at different temperatures are between 0 and 20 which indicates the physical adsorption process.

Table 3
Thermodynamic parameters for LBB on *S. cerevisiae*

| $T$ (K) | $\Delta G°$ (kJ/mol) | $\Delta S°$ (J/mol k) | $\Delta H°$ (kJ/mol) |
|---|---|---|---|
| 298 | −5.3 | 40.9 | −6.8 |
| 303 | −5.4 | | |
| 313 | −5.9 | | |
| 323 | −6.5 | | |

### 3.8. Fourier-transform infrared spectrometry

Graphs of Fourier-transform infrared spectrometry (FT-IR) analysis of pretreated *S. cerevisiae* cell before and after biosorption. Further study based on the biosorption phenomenon of LBB on heat pretreated yeast cells is FT-IR. The functional groups of organic materials which allowed for the binding of the dye to the cell of the yeast cell are studied in the frequency range of 500 to 4,000 cm$^{-1}$ (Fig. 6). FT-IR is carried out on yeast cell strain before and after biosorption studies. Yeast biomass was dried and used for FT-IR analysis. The spectra region consists of a set of peaks. This analysis further affirmed the presence of binding sites available for the biosorption and these binding sites (functional groups) in relation to the biosorption occurred and to change in the chemical composition. The biosorption by heat pretreated cells of *S. cerevisiae* may be due to the presence of these observed active groups on cell surface such as lipids, amino acids, polysaccharides, phosphoryl and carboxyl groups and other cellular components of the organism. From Fig. 7, we could find that the most significant bands were in the regions of 3,448, 2,958, 1,629, 1,560 and 1,137 cm$^{-1}$. A weak absorption at 2,958 cm$^{-1}$ was usually ascribed to the aliphatic groups (asymmetrical and symmetrical stretch of $CH_3$). The sharp band located in 1,620–1,630 can be said to correspond to an aromatic carbon or

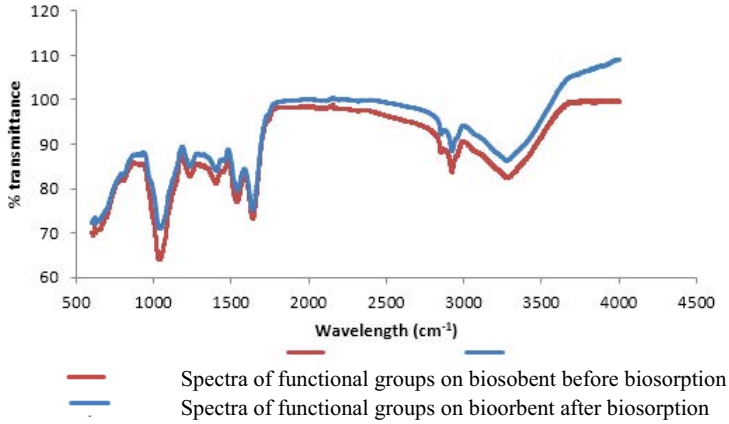


Fig. 6. Fourier-transform infrared spectrometry (FT-IR) of *S. crevisiae* before and after biosorption.

carbonyls (a stretch of C=C in aromatic rings), according to literature. The band at 1,137 $cm^{-1}$ may belong to C–O stretching in alcohol or ether or hydroxyl groups. The above results indicated that functional groups on the surface of Baker's yeast affected the adsorption process [31].

## 4. Conclusion

The capacity of *S. cerevisiae* to remove LBB dye from an aqueous solution was studied by means of evaluation of the parameters: initial dye concentration, biosorbent dosage, pH of the dye solution, and temperature. Additionally, biosorption kinetics, isotherm, and thermodynamic studies have also been established. The results obtained in this research clearly highlight the potential of heat pretreated yeast powder, a cheap material, as a possible biosorbent for the evacuation of textile industry effluent. The thermodynamic analysis of the experimental data suggested the process was feasible and spontaneous. It also suggests that the adsorption was controlled by the physisorption process as evidenced by the *E*-value which is less than 8 kJ/mol obtained in the D–R isotherm model. Although the literature comprises numerous studies on the removal of different dye through biosorption with biosorbent materials, no study had been conducted using *S. cerevisiae* for the removal of LBB with further addition of thermodynamic study for the understanding of adsorption mechanism and process. This study was critical based on the fact that the raw material used can be made available easily, easy to prepare, and environmentally safe. Thus, this study shows that *S. cerevisiae* justifies consideration as biomass that can be used in the treatment of wastewater containing dyes and it may be considered as an alternative to more expensive materials such as activated carbon.

## Acknowledgment

The authors thank the laboratory assistants of the laboratories the experiments were carried out for their support during the period of the research.

## Symbols

$Q_e$ — Adsorption capacity (mg/g) at the equilibrium
$Q_t$ — Adsorption capacity (mg/g) at time *t*
$C_0$ — Initial concentration of the dye in the solution, mg/L
$C_e$ — Concentration of the dye in the solution at equilibrium, mg/L
$C_t$ — Concentration of the dye in the solution at time *t*, mg/L
$V$ — Volume of the solution, L
$m$ — Dry weight of the biosorbent, g
$q_e$ — Measure of sorbate adsorbed per gram of the adsorbent at equilibrium, mg/g
$q_m$ — Maximum monolayer sorption capacity, mg/g
$b$ — Langmuir isotherm constant, L/mg
$R_L$ — Separation factor
$K_F$ — Freundlich isotherm steady (mg/g) pseudo-second-order constant
$n$ — Adsorption force
ε — Polanyi potential
$q_{D–R}$ (mol/g) — Maximum adsorption limit of D–R model
β ($mol^2/kJ^2$) — Coefficient relating to the mean free energy of adsorption of D–R model
$R$ — Ideal gas constant, J/mol K
$T$ — Absolute temperature, K
$A_T$ — Temkin isotherm constant, L/g
$b_T$ — Temkin constant
$k_1$ — Pseudo-first-order rate constant, $min^{-1}$
$k_2$ — Pseudo-second-order rate constant, $min^{-1}$
$h$ (mg/g min) — Initial sorption rate
$k_d$ (mg/g $min^{1/2}$) — Rate constant of Weber–Morris model
$\Delta G$ – Free energy change
$\Delta H$ – Enthalpy change
$\Delta S$ – Entropy change

## References

[1] B.R. Babu, A.K. Parande, S. Raghu, T.P. Kumar, Cotton textile processing: waste generation and effluent treatment, J. Cotton Sci., 11 (2007) 141–153.
[2] O. Ozdemir, B. Armagan, M. Turan, M.S. Celik, Comparison of the adsorption characteristics of azo-reactive dyes on mezoporous minerals, Dyes Pigm., 62 (2004) 49–60.
[3] J.B. Donnet, E. Papirer, Effect on surface reactivity of carbon surface by oxidation with ozone, Bull. Soc. Chim. Fr., (1965) 1912.

[4] C.J. Ogugbue, T. Sawidis, Bioremediation and detoxification of synthetic wastewater containing triarylmethane dyes by *Aeromonas hydrophila* isolated from industrial effluent, Biotechnol. Res. Int., 2011 (2011) 1–11, doi: 10.4061/2011/967925.
[5] M.F. Rahman, N.J. Ara, M.M. Uddin, M.Z. Sultan, Toxic effects of Levafix blue CA and Levafix amber CA reactive dyes on liver and kidney in mice, Int. J. Food Sci. Nutr., 6 (2017) 187–193.
[6] X. Hao, L. Quac, J. Korah, W.A. Spieker, J.R. Regalbuto, The control of platinum impregnation by PZC alteration of oxides and carbon, J. Mol. Catal. A: Chem., 219 (2004) 97–107.
[7] H.N. Bhatti, Y. Safa, S.M. Yakout, O.H. Shair, M. Iqbal, A. Nazir, Efficient removal of dyes using carboxymethyl cellulose/alginate/polyvinyl alcohol/rice husk composite: adsorption/desorption, kinetics and recycling studies, Int. J. Biol. Macromol., 150 (2020) 861–870.
[8] Y. Safa, S.R. Tariq, H.N. Bhatti, M. Sultan, I. Bibi, S. Nouren, Synthesis and characterization of sugarcane bagasse/zinc aluminium and apple peel/zinc aluminium biocomposites: application for removal of reactive and acid dyes, Membr. Water Treat., 9 (2018) 301–307.
[9] S. Noreen, H.N. Bhatti, M. Iqbal, F. Hussain, F.M. Sarim, Chitosan, starch, polyaniline and polypyrrole biocomposite with sugarcane bagasse for the efficient removal of Acid Black dye, Int. J. Biol. Macromol., 147 (2020) 439–452.
[10] F. Kargi, S. Ozmihci, Biosorption performance of powdered activated sludge for removal of different dyestuffs, Enzyme Microb. Technol., 35 (2004) 267–271.
[11] L.F. Cusioli, C.D.O. Bezerra, H.B. Quesada, A.T. Alves Baptista, L. Nishi, M.F. Vieira, R. Bergamasco, Modified Moringa oleifera Lam. Seed husks as low-cost biosorbent for atrazine removal, Environ. Technol., 42 (2021) 1092–1103.
[12] J. Choi, J.Y. Lee, J.S. Yang, Biosorption of heavy metals and uranium by starfish and *Pseudomonas putida*, J. Hazard. Mater., 161 (2009) 157–162.
[13] A.M. Subasri, N. Mani, Equilibrium, kinetic and thermodynamic study on Rhodamine-B removal from aqueous solution using activated *Corchorus olitorius-L* leaves, Int. J. Plant Anim. Environ. Sci., 5 (2015) 208–218.
[14] T. Madrakian, A. Afkhami, M. Ahmadi, H. Bagheri, Removal of some cationic dyes from aqueous solutions using magnetic-modified multi-walled carbon nanotubes, J. Hazard. Mater., 196 (2011) 109–114.
[15] N.M. Mahmoodi, B. Hayati, M. Arami, C. Lan, Adsorption of textile dyes on pine cone from colored wastewater: kinetic, equilibrium and thermodynamic studies, Desalination, 268 (2011) 117–125.
[16] M.S. Mahmoud, Decolorization of certain reactive dye from aqueous solution using Baker's Yeast (*Saccharomyces cerevisiae*) strain, HBRC J., 12 (2016) 88–98.
[17] A. Ozer, G. Akkaya, M. Turabik, The removal of Acid Red 274 from wastewater: combined biosorption and biocoagulation with *Spirogyra rhizopus*, Dyes Pigm., 71 (2006) 83–89.
[18] H.A. Erkurt, M. Özyurt, A. Özer, Adsorption by active and inactive *Aspergillus oryzae*: batch studies, Adsorpt. Sci. Technol., 30 (2012) 317–330.
[19] Z. Aksu, G.A. Donmez, Comparative study on the biosorption characteristics of some yeast for Remazol Blue reactive dye, Chemosphere, 50 (2003) 1075–1083.
[20] K. Kumar, M.G. Dastidara, T.R. Sreekrishna, Effect of process parameters on aerobic decolourization of reactive azo dye using mixed culture, World Acad. Sci. Eng. Technol., 58 (2009) 962–965.
[21] D. Sara, K.S. Tushar, Removal of anionic dye Congo red from aqueous solution by raw pine and acid-treated pine cone powder as adsorbent: equilibrium, thermodynamic, kinetics, mechanism and process design, Water Res., 46 (2012) 1933–1946.
[22] Y. Fu, T. Viraraghavan, Removal of Acid Blue 29 from an aqueous solution by *Aspergillus niger*, Am. Assoc. Text. Chem. Color. Rev., 1 (2001) 36–40.
[23] L. Morais, O. Freitas, E. Gancolves, L. Vaskancelos, C. Gonzalez, Reactive dyes removal from wastewaters by adsorption on eucalyptus bark: variables that define the process, Water Res., 33 (1999) 979–988.
[24] A.A. Ragheb, K. Haggag, I.A. Rekaby, A.A. Shahin, Bio-discharge printing on cotton knitted fabrics using enzyme and brewer's yeast, Res. J., 9 (2013) 205–225.
[25] B. Benguella, H. Benaissa, Cadmium removal from aqueous solutions by chitin: kinetic and equilibrium studies, Water Res., 36 (2002) 2463–2474.
[26] S. Kahraman, D. Asma, S. Erdemoglu, O. Yesilada, Biosorption of copper(II) by live and dried biomass of the white rot fungi *Phanerochaete chrysosporium* and *Funalia trogii*, Eng. Life Sci., 5 (2005) 72–77.
[27] K. Kumari T.E. Abraham, Biosorption of anionic textile dyes by nonviable biomass of fungi and yeast, Bioresour. Technol., 98 (2007) 1704–1710.
[28] M.I. Tempkin, V. Pyzhev, Kinetics of ammonia synthesis on promoted iron catalyst, Acta Phys. Chim., 12 (1940) 327–356.
[29] Y.S. Ho, G. McKay, Pseudo-second order model for sorption processes, Process Biochem., 34 (1999) 451–465.
[30] A. Özcan, E.M. Öncü, A.S. Özcan, Kinetics, isotherm and thermodynamic studies of adsorption of Acid Blue 193 from aqueous solutions onto natural sepiolite, Colloids Surf., A, 277 (2006) 90–97.
[31] M. Liu, F. Dong, W. Zhang, X. Nie, H. Wei, S. Sun, D. Wang, Contribution of surface functional groups and interface interaction to biosorption of strontium ions by *Saccharomyces cerevisiae* under culture conditions, RSC Adv., 7 (2017) 50880–50888.